

III-V semiconductor waveguides for photonic functionality at 780 nm

Jessica O. Maclean, Mark T. Greenaway, Richard P. Campion, Tadas Pyragius, T. Mark Fromhold, Anthony J. Kent and Christopher J. Mellor

School of Physics and Astronomy, University of Nottingham, University Park, Nottingham, NG7 2RD, United Kingdom

ABSTRACT

Photonic integrated circuits based on III-V semiconductor polarization-maintaining waveguides were designed and fabricated for the first time for application in a compact cold-atom gravimeter^{1,2} at an operational wavelength of 780 nm. Compared with optical fiber-based components, semiconductor waveguides achieve very compact guiding of optical signals for both passive functions, such as splitting and recombining, and for active functions, such as switching or modulation.

Quantum sensors, which have enhanced sensitivity to a physical parameter as a result of their quantum nature, can be made from quantum gases of ultra-cold atoms. A cloud of ultra-cold atoms may start to exhibit quantum-mechanical properties when it is trapped and cooled using laser cooling in a magneto-optical trap, to reach milli-Kelvin temperatures. The work presented here focuses on the design and fabrication of optical devices for a quantum sensor to measure the acceleration of gravity precisely and accurately. In this case the cloud of ultra-cold atoms consists of rubidium (⁸⁷Rb) atoms and the sensor exploits the hyperfine structure of the D1 transition, from an outer electronic state of $5^2S_{1/2}$ to $5^2P_{3/2}$ which has an energy of 1.589 eV or 780.241 nm.

The short wavelength of operation of the devices dictated stringent requirements on the Molecular Beam Epitaxy (MBE) and device fabrication in terms of anisotropy and smoothness of plasma etch processes, cross-wafer uniformities and alignment tolerances. Initial measurements of the optical loss of the polarization-maintaining waveguide, assuming Fresnel reflection losses only at the facets, suggested a loss of 8 dB cm^{-1} , a loss coefficient, α , of $1.9 (\pm 0.3) \text{ cm}^{-1}$.

Keywords: semiconductor, waveguide, AlGaAs, polarization, cold atoms, Rubidium, photonic circuit, gravimeter

1. INTRODUCTION

On-chip optoelectronic systems offer full optical functionality if they can integrate active and passive devices such as waveguides, sources, detectors, amplifiers, switches, modulators and optical parametric devices.

Many quantum sensors would become portable with an integrated optic approach to optical functionality and would give the additional benefits of stable alignment of components and lower weight and cost. Modest functionality can greatly impact the stability and cost of portable experiments.

Quantum sensors using cold atoms rely on atomic transitions at specific wavelengths, such as the ^{87}Rb D1 transition line at 780.241 nm, in combination with fiber-interfaced components and free-space components to guide light into and out of an experimental vacuum chamber. The acceleration of gravity was measured with an accuracy of 1 part in 10^7 using an experimental scheme³ combining atom interferometry and Bloch oscillations and a short falling distance for the ultra-cold atoms of 0.8 mm. The research described here aims to develop a III-V-based integrated optic technology at 780 nm for compact, ultra-cold atom-based quantum sensors

Semiconductor devices benefit from high resolution fabrication techniques and high quality single crystal substrates with atomically-flat surfaces. Semiconductors with a direct bandgap can absorb and emit light efficiently as well as guide light. In the III-V semiconductor system based on indium phosphide (InP), active and passive devices are integrated on wafer for commercial components at telecommunications wavelengths. However, for wavelengths shorter than $1\ \mu\text{m}$ an alternative alloy system must be used⁴.

The III-V semiconductor alloys gallium arsenide (GaAs) and aluminum arsenide (AlAs) have low lattice mismatch ($(\delta a)/a \sim 10^{-4}$ where a is the GaAs lattice parameter) enabling epitaxy free of misfit dislocations for a wide range of compositions and growth temperatures. The refractive index difference, δn , between GaAs and AlAs is 0.8 at room temperature. The bandgap at room temperature of GaAs corresponds to 870 nm and that of AlAs corresponds to 570 nm. Therefore the $\text{Al}_x\text{Ga}_{(1-x)}\text{As}$ semiconductor alloy has great potential for guiding light compactly in Rb-based cold atom experiments at 780 nm.

On-wafer photonic integrated circuits may need to be interfaced to an external laser via an optical fiber. Particularly in the case of an existing cold atom experimental set-up, where the (narrow linewidth) master laser, repumper and spectroscopy lasers may be fiber-interfaced, any photonic integrated circuit needs to be aligned precisely to the fundamental mode in the fiber. Good optical overlap between the fiber mode and the waveguide mode for low coupling loss is required. Such connections are typically made by curing an epoxy in an active alignment set-up to maximize transmission into the chip. This is an expensive approach with regards to testing chips in a development program although is acceptable for the packaging of a completed batch of fiber-interfaced modules.

2. METHODOLOGY

The application to the cold atom sensor stipulates a reasonably low-loss, single mode, polarization-maintaining waveguide for 780 nm wavelength. For a compact sensor system the insertion loss of the component is the most important parameter and includes the input and output coupling losses. The long-term vision of the iSense^{1,2} program is a modular, scalable and portable quantum technology family based on the confinement of cold atoms using an optical lattice, adaptable to a wide variety of applications in diverse working environments.

The sensors of today are almost entirely based on classical working principles, e.g. falling corner cubes for gravity measurements and in standard applications these have a low cost for significant benefit. However for extremely high precision measurements these devices become impractical due to rapidly increasing requirements on material and manufacturing tolerances. The fundamental physical properties of the atoms themselves ensure reproducibility and consistency for a quantum sensor which uses atoms as probes. A highly-sensitive cold-atom gravimeter sensor functionality was achieved on the scale of an optical table³ but

the iSense gravimeter will use semiconductor-chip-sized optical circuits to increase compactness. The waveguide loss consists of several contributions including Fresnel losses at waveguide-air interfaces, facet imperfections, intrinsic material losses from free carrier absorption and any unintentional deep levels (which act as centers for non-radiative recombination) as well as any scattering losses from surface roughness, morphological defects or surface residues.

The epitaxial structure was designed using Optiwave beam propagation mode software in the GaAs / Al_xGa_(1-x)As semiconductor system and grown using elemental sources of Ga, Al and As, on semi-insulating GaAs (100) 75 mm diameter substrates by in-house Molecular Beam Epitaxy (MBE). Growth took place in a Veeco Gen III MBE reactor equipped with reflection High Energy Electron Diffraction (RHEED) in-situ surface reconstruction monitoring, and BandIT temperature control systems. Optimization of material quality consisted of controlling the relative fluxes (of Ga, Al, As) and growth rates of Al_xGa_(1-x)As alloys. Growth temperatures and flux ratios were optimized to achieve the designed composition with atomically smooth semiconductor interfaces, low defect density and low unintentional dopant concentrations. Lattice parameters were measured using X-ray diffraction (Philips X'Pert Materials Research Diffractometer) and used to verify Al composition based on a previously published model⁴.

In the GaAs / AlAs III-V semiconductor material system it is well established⁵ that oxygen present in the epitaxy reactor during growth can be incorporated into the structure where it leads to a strong reduction of the non-radiative recombination lifetimes of the electrons and holes. Previous studies⁶ of material quality for 850 nm laser / waveguide integration showed a clear correlation between waveguide optical loss and high unintentional dopants and low photoluminescence (PL) lifetimes, measurable oxygen concentrations changing the PL lifetime from around 6 ns to around 2 ns.

The PL lifetime measurements presented here were made using a frequency-doubled Ti-sapphire laser outputting 720nm/1.73eV pulses of 100fs duration and 82MHz repetition rate and power ~3.5mW. Light was collected and focused using parabolic mirrors. An Oriel 77200 monochromator was used to isolate light wavelengths, which were collected using a Becker and Hickl PMH-100-4 photomultiplier tube and counted using a Becker and Hickl SPC-360 board. The sampling interval was 3ps and time resolution was ~150ps. Secondary ion mass spectrometry (SIMS) measurements were performed at Loughborough Surface Analysis Ltd., UK.

In order to achieve low free carrier absorption for propagation of 780 nm light in the waveguide core, the composition of the semiconductor was selected to have a bandgap which exceeded the photon energy of 1.59 eV. The number of modes which can propagate in such a waveguide is determined by the effective refractive index of each mode as compared to the refractive index of the cladding layer. In order to make the waveguide single mode, a method⁸ was used which was originally reported to filter the modes in a rib waveguide. The waveguide was designed so that only the fundamental mode has an effective refractive index that is higher than the lower cladding layer. All modes other than the fundamental mode leak strongly into the substrate. The differences in refractive index for each layer (and consequently the changes in Al concentration) are therefore required to be small since the effective mode indices for the higher order modes are generally close to that of the fundamental mode. Hence very precise compositional control over the growth process is required. However, the data on the refractive index for Al_xGa_(1-x)As as a function of composition is not comprehensive and therefore this work is also means of verifying the functional dependence of refractive index. A suggested functional dependence⁹ was identified which combined the available empirical data with numerical simulations.

One disadvantage of optical fibers is their tendency to rotate the plane of polarization between input and output and for the polarization to be sensitive to stress in the fiber. For a cold atoms experiment, the polarization needs to be preserved accurately as atomic transitions with specific circular polarizations are

measured and any rotation of the linear polarization input to the wave plates will lead to poorer signal-to-noise ratios in the atomic spectroscopy. The waveguides were designed to be polarization-filtering by manipulating the effective refractive indices for transverse electric (TE) and transverse magnetic (TM) modes in the structure of the waveguide. This technique was used in a device described previously¹⁰ but has not, to our knowledge, been used in the GaAs / Al_xGa_(1-x)As system before.



Figure 1. Simulation of a single mode polarization-maintaining waveguide for 780 nm functionality. The greyscale shading indicates contours of intensity.

It is challenging to measure the optical loss of very small waveguide structures when the optical mode size within the launch fiber is larger than the cross-section of the waveguide. This is because optical losses occur as a result of imperfect mode overlap between the fiber mode and the waveguide mode, divergence of the light at the tapered fiber output, as a result of Fresnel reflection at the air / semiconductor interfaces (on entering the waveguide and at the output to the guide), and the mode overlap between the diverging light from the waveguide and the numerical aperture of the receiving microscope. Misalignment of end facets with respect to the input light and output receiver axis will also incur some paraxial and reflection loss. Finally, light will be reflected at the surface of the chip and also captured by the camera, as well as entering the substrate adding light output to the camera and necessitating an iris to stop down the received light to exclude all but the waveguide output mode. The coupling and Fresnel losses could be reduced by active alignment of the input and output using microlenses and coating the facet with an anti-reflection coating respectively.

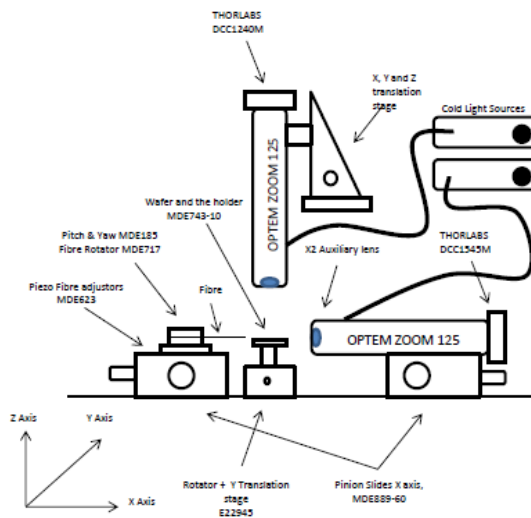


Figure 2. Newly-assembled optical test set-up for waveguide testing showing tapered polarization-maintaining input fiber, translation stage for sample alignment and zoom microscope with camera sensor for detecting output light.

An optical test bench was set up to measure the optical loss of the waveguides. Light at 780 nm was coupled from a homemade diode laser¹¹, capable of delivering up to 1 mW power, into a single mode tapered fiber on a 6-axis positioner with a rotatable fiber stage, manufactured by Elliott Scientific (see Fig. 2). The waveguide device was positioned on a 2-axis stage and the output light was received via a microscope to a camera or power meter. An inspection system allowed for the plan view of the waveguides and another for the output of the waveguides. Fine motor control of the fiber is achieved using a 3-axis open loop piezo controller and a high precision adjustable stage for pitch and yaw.

The output light was imaged by a CMOS camera focused using a zoom microscope and the output power was measured in orthogonal polarizations. The Fresnel reflections from the cleaved ends of the waveguides cause the waveguide to act as a lossy Fabry-Perot cavity. Assuming the Fresnel reflections and coupling are not, to first order, temperature sensitive, the loss of the waveguide can be determined from the oscillation in output power as the cavity length is altered. The length of the cavity was altered by changing the temperature of the substrate by around 10K. This method¹² is suitable for cavities which have a quality factor of 10 – 100 and because it is a ratio method, it is not necessary to know the light power captured by the waveguide (providing there is no measurable change in the coupling efficiency on heating the fiber). Input power to the tapered fiber was 0.34 mW but it is probable that only a fraction of this was captured by the high contrast polarization-maintaining narrow waveguide.

3. RESULTS

The MBE-grown material was found to have a low surface defect density and to be of high structural quality. X-ray diffraction rocking curve widths for the (004) reflections showed the GaAs substrate and a 50% AlGaAs layer to have similar values of 0.019 degrees (see Fig. 3). The strength of the intensity oscillations is indicative of smooth upper and lower interfaces.

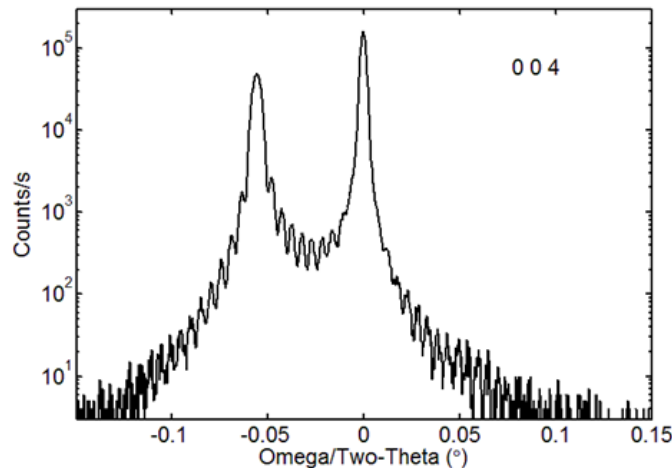


Figure 3. XRD intensity as a function of angle omega referenced to 2-theta for the (004) diffraction peaks for the GaAs substrate and a 1 μm thick layer of 50% AlGaAs.

Photoluminescence lifetime test structures gave a minority carrier non-radiative lifetime of 5.8 ns (see Fig. 4), a result considered to be an indicator of a high material quality at this wavelength. The non-radiative lifetime improved by a factor of 10 as a result of improved growth conditions during the research program.

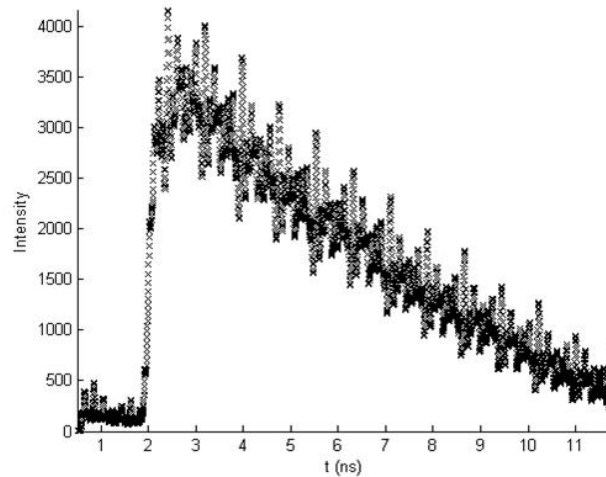


Figure 4. Non-radiative decay of photoluminescence for a GaAs /AlGaAs superlattice test structure showing a non-radiative lifetime of 5.8 ns.

SIMS measurements suggested that unintentional oxygen concentrations did not exceed $5 \times 10^{16} \text{ cm}^{-3}$ in $\text{Al}_{0.3}\text{Ga}_{0.7}\text{As}$ for structures grown under optimal growth conditions.

The plasma etching of arsenides requires chloride ions provided by chlorine, boron trichloride or silicon tetrachloride sources. Physical etching also occurs by neutral species in the etch plasma such as argon, nitrogen or non-ionized chlorine molecules in the plasma. The etching parameter space was explored in the many etching parameters (RF and inductively-coupled plasma (ICP) power, sample temperature, total pressure, partial pressures etc.) to find conditions under which there was sufficient etch selectivity between the semiconductor and photoresist, sufficient sidewall smoothness for the waveguides, and sufficient anisotropy to obtain near-vertical sidewalls to give the waveguide a rectangular cross-section. A further requirement for photonic circuits where waveguides need to guide light over several cm of length is high cross-wafer uniformity so that the height of the waveguide is the same across the whole semiconductor wafer. Plasma etching of the GaAs / $\text{Al}_x\text{Ga}_{(1-x)}\text{As}$ waveguides was optimized using ICP etching with a Corial 200IL plasma etching system and a gas mixture of SiCl_4 / Ar at a substrate temperature of 0°C . Sidewall angle was of the order of $(70-80)^\circ$ as measured using Scanning Electron Microscopy (SEM). It is possible that this could be further improved but simulations suggest that this should contribute an additional loss of no more than 0.2 dB cm^{-1} . Etching control to a precise depth was achieved by laser reflectometry at 670 nm which showed characteristic interference oscillations of the reflected laser intensity according to the wavelength of the light in the semiconductor layer. Careful choice of the monitoring wavelength and design of the polarization-maintaining waveguide structure resulted in a depth precision of about 50 nm in the etch depth (see Fig. 5). Following careful sample cleaning, optical microscopy examination revealed uniformly smooth waveguides of constant width (see Fig. 5).

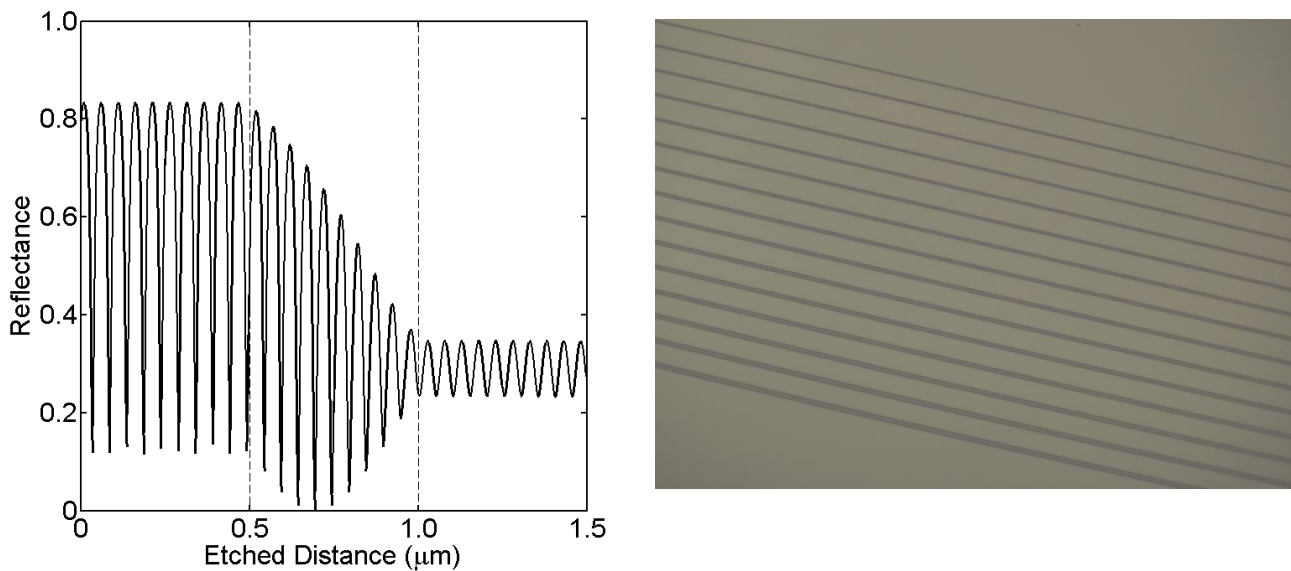


Figure 5. Simulation of laser reflectometry data during AlGaAs etching of the fine waveguide structure. Depths of up to 6 μm may be etched with an accuracy of 50 nm at the University of Nottingham. Optical microscopy (right) (magnification x100) of simple straight waveguides spaced 50 μm apart after fine waveguide etching and solvent cleaning.

The 75 mm diameter wafer was held in the center of a cooled stage on a quartz sample platen. Using a substrate temperature of 0°C, the variation in the etch depth from the center to edge of the sample was 6%.

An optical test bench was set up to measure the optical loss of the waveguides. Light at 780 nm was coupled from a homemade diode laser¹¹, capable of delivering up to 1 mW power, into a single mode tapered fiber on a 6-axis positioner with a rotatable fiber stage, manufactured by Elliott Scientific (see Fig. 2). The waveguide device was positioned on a 2-axis stage and the output light was received via a microscope to a camera or power meter. An inspection system allowed for the plan view of the waveguides and another for the output of the waveguides. Fine motor control of the fiber is achieved using a 3-axis open loop piezo controller and a high precision adjustable stage for pitch and yaw.

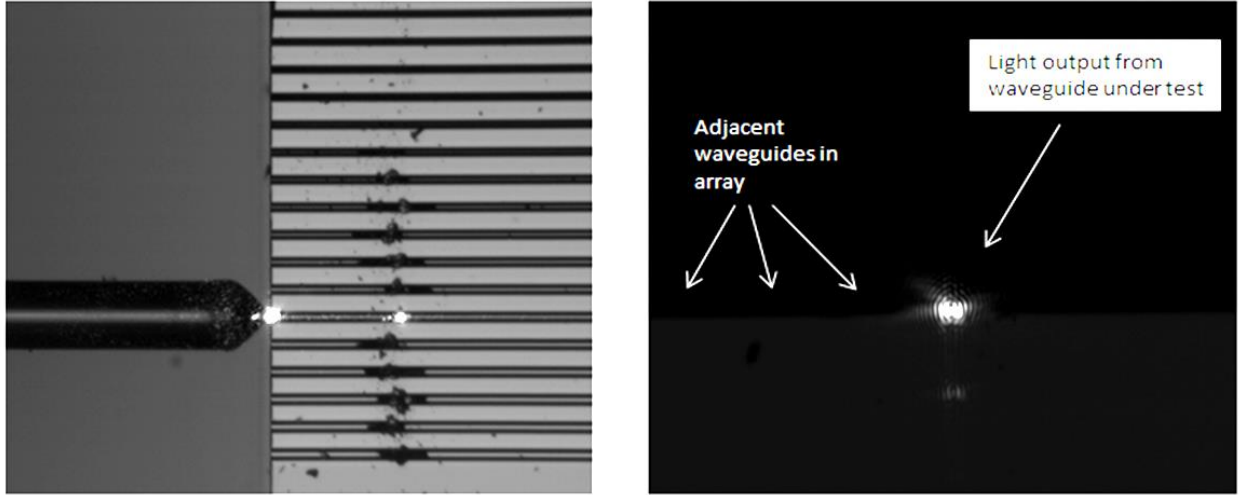


Figure 6. Plan view and output images of the sample 737 under test showing the optical fiber launching 780 nm laser light into a 7.5 μm wide waveguide in the waveguide array. The waveguide was damaged by tweezers so that some of the light is visible refracting out of the top surface of the waveguide, as a bright spot. Most of the light reached the end of the waveguide chip several mm away and the right hand image shows the mode of the output light detected by the camera sensor.

An example of wafer testing is shown in Fig. 6 with a plan view image of the tapered fiber and waveguide chip alongside the image of the end facets of the output of the waveguides. Optical loss was measured for a 3.5 μm wide, 1.05 cm long waveguide by inputting 23 nW 780 nm laser light (laser current 40 mA and maintained at 21.1 $^{\circ}\text{C}$) and radiatively heating it from above for 1800 s to produce a temperature rise of approximately 10 $^{\circ}\text{C}$. The output power intensity on cooling was then monitored for more than one hour. As the cavity length reduced on cooling, intensity oscillations with a contrast of 0.106 were observed. Assuming a Fresnel coefficient of 0.286, this corresponded to a loss coefficient, α of 1.9 (± 0.2) cm^{-1} , or approximately 8 dB cm^{-1} .

4. DISCUSSION

There are few reports in the literature of waveguide loss for $\text{Al}_x\text{Ga}_{(1-x)}\text{As}$ -based waveguides grown by MBE at near-infra-red wavelengths and no previous reports of polarization-maintaining waveguides.

The optical loss of $\text{Al}_x\text{Ga}_{(1-x)}\text{As}$ waveguides¹³ of 4 μm square cross-section with both core ($x=77.5\%$, $n=3.145$) and cladding ($x=79.5\%$, $n=3.155$) layers grown epitaxially by Molecular Beam Epitaxy (MBE) was measured to have a loss coefficient, $\alpha = 1.07$ (± 0.06) cm^{-1} or about 4.6 dB cm^{-1} . Having an effective refractive index of 3.50 (± 0.04), these guides had a maximum intrinsic finesse of 92 when high-reflection-coated at one end. This optical propagation loss included any absorption processes in the material, any scattering losses from surface or interface roughness and any inhomogeneities in the bulk semiconductor and could possibly have been reduced also by optimizing the Al composition of the waveguides. These waveguides were designed for use within the experimental chamber of an ultra- cold atom experiment to create a cavity with an enhanced coupling factor between cold atom and electric field in an air gap.

A very low loss result¹⁴ of less than 0.1dB/cm at a wavelength of 830nm was reported for AlGaAs waveguides of width 2-5 μm grown by Metalorganic Vapor Phase Epitaxy (MOVPE) using purified arsine in hydrogen as the Group V precursor and a high V-III ratio during growth. Waveguides were etched using chemical wet-

etching through the top cladding and core to a depth of 2 μm . The waveguide core had an Al fraction of 0.35, the cladding an Al fraction of 0.4 and the waveguides were single mode at a width of 2.4 microns. Background carrier concentration was measured by capacitance-voltage (CV-) profiling and was $(1-6) \times 10^{16} \text{ cm}^{-3}$ n- or p-type depending on growth conditions. The low loss samples had a superlattice buffer layer, low surface defect density and purified arsine using a eutectic liquid metal bubbler to reduce oxygen and water impurities and the importance of these was clearly shown by comparison with other samples.

Thus when measured at wavelengths close to 800 nm, and when grown by different growth techniques, the optical loss measurements reported differ significantly for non-polarization-maintaining waveguides. Further studies of waveguides grown using MBE and MOVPE and processed identically are required to better understand the causes of optical loss. It is possible that there are different band edge states present depending on both the growth conditions and the precursor sources. Furthermore, a comparison of non-polarization-maintaining and polarization-maintaining waveguides for the 780 nm wavelength would assist in clarifying the causes of optical loss.

In practice, in a compact optical system, the total insertion loss and functionality of the component are of prime importance, particularly if sufficient laser power or optical amplification is available.

5. CONCLUSIONS

Semiconductor rib waveguides were designed for single-mode propagation of 780 nm light, grown by MBE, applicable to cold atom sensors based on atomic transitions of ^{87}Rb for the first time using precise optical lithography and ICP etching.

Waveguides were simulated using the effective index method and the software tool, Optiwave, to determine a structure for which there was low loss propagation for the fundamental mode but attenuation for the higher order modes. Furthermore, the waveguide was designed to propagate the TE mode only.

The epitaxial structure was grown in the GaAs / $\text{Al}_x\text{Ga}_{(1-x)}\text{As}$ semiconductor system using elemental sources of Ga, Al and As, on semi-insulating GaAs 75 mm diameter substrates by in-house MBE. Growth temperatures and flux ratios were optimized for designed composition, atomically smooth semiconductor interfaces, low defect density and low unintentional dopant concentrations. Lattice parameters were measured using XRD and used to verify Al composition and revealed the material to be of high structural quality. PL lifetime test structures, grown within a few growth runs of the waveguide growth structures themselves, gave a minority carrier non-radiative lifetime of 5.8 ns, a result considered to be an indicator of a high material quality at this wavelength. Secondary ion mass spectrometry (SIMS) measurements suggested that unintentional Oxygen did not exceed a concentration of $5 \times 10^{16} \text{ cm}^{-3}$.

Wafers were processed as whole wafers using masks designed in-house. Precise alignment and cross-wafer uniformity were achieved in order to make photonic waveguide circuits of various sizes. Waveguide optical loss was measured using 780 nm laser light from a diode laser input to a tapered fiber and precisely aligned in free space to the input of the semiconductor waveguide. An optical loss at 780 nm was measured which was sufficiently low to demonstrate that AlGaAs waveguides are promising for application to the design of compact cold atom experimental sensors. A comparison of polarization-maintaining and non-polarization-maintaining waveguide losses is required to clarify the causes of optical loss.

6. ACKNOWLEDGMENTS

We wish to thank the EU Grant Agreement no. 250072 “iSense” for funding and to acknowledge the expertise of R. E. L. Powell in the measurements of photoluminescence lifetimes.

REFERENCES

- [1] De Angelis, M., Angonin, M.C., Beaufiles, Q., Becker, Ch., Bertoldi, A., Bongs, K., Boudel, T., Bouyer, P., Boyer, V., Dorscher, S., Duncker, H, Ertmer, W., Fernholz, T., Fromhold, T.M., Herr, W., Kruger, P., Kurbis, Ch, Mellor, C.J., Pereira Dos Santos, F., Peters, A., Poli, N., Popp, M., Prvedelli, M., Rasel, E.M., Rudolph, J., Schreck, F., Sengstock, K., Sorrentino, F., Stellmer, S., Tino, G.M., Valenzuela, T., Wendrich, T.J., Wicht, A., Windpassinger, P. and Wolf, P., “iSense: A Portable Ultracold-Atom-Based Gravimeter”, *Procedia Computer Science*, 7 334-336 (2011).
- [2] <http://www.isense-gravimeter.eu/>
- [3] R. Charriere, M. Cadoret, N. Zahzam, Y. Bidel and A. Bresson, “Local gravity measurement with the combination of atom interferometry and Bloch oscillations”, *Physical Review A*, 85, 013639 (2012).
- [4] Wasilewski, Z.R., Dion, M.M., Lockwood, D.J., Poole, P., Streater, R.W. and SpringThorpe, A.J., “Composition of AlGaAs”, *Journal of Applied Physics*, 81 1683 (1997).
- [5] Foxon, C.T., Clegg, J.B., Woodbridge, K., Hilton, D., Dawson, P. and Blood, P., “The effect of the oxygen concentration on the electrical and optical properties of AlGaAs films grown by MBE”, *Journal of Vacuum Science and Technology. B*, 3 539 (1985).
- [6] Balmer, R.S., Martin, T., Kane, M.J., Maclean, J.O., Whitaker, T.J., Ayling, S.G., Calcott, P.D.J., Houlton, M., Newey, J.P. and O’Mahony, S.J., “Integrated laser/waveguide by shadow-masked selective area epitaxy using chemical beam epitaxy (CBE),” *Journal of Crystal Growth*, 209, 486-491 (2000).
- [7] Heaton, J.M., Bourke, M.M., Jones, S.B., Smith, B.H., Hilton, K.P., Smith, G.W., Birbeck, J.C.H., Berry, G., Dewar, S.V. and Wight, D.R., “Optimization of Deep-etched, Single-mode GaAs / AlGaAs Optical Waveguides using Controlled Leakage into the Substrate”, *Journal of Lightwave Technology*, 17(2), 267-281 (1999).
- [8] Sadao Adachi, “GaAs, AlAs and Al_xGa_{1-x}As: Material parameters for use in research and device applications”, *Journal of Applied Physics*, 58 (R1) 1-29 (1985).
- [9] Rahman, B.M.A., Obayya, S.S.A., Boonthittanont, W. and Heaton, J.M., “Novel Polarization-Maintaining Semiconductor Waveguide”, *IEEE Photonics Technology Letters*, 16 807-809 (2004).
- [10] Wieman, C.E. and Hollberg, L., “Using diode lasers for atomic physics”, *Review of Scientific Instruments*, 62(1) 1-20 (1991).
- [11] Tittelbach, G, Richter, B. and Karthe, W., “Comparison of three transmission methods for integrated optical waveguide propagation loss measurement”, *Pure and Applied Optics*, 2 683-706 (1993).
- [12] Gleyzes, S., El Amili, A., Cornelussen, R.A., Lalanne, P., Westbrook, C.I., Aspect, A., Estve, J., Moreau, G., Martinez, A., Lafosse, X., Ferlazzo, L., Harmand, J. C., Mailly, D. and Ramdane, A., “Towards a monolithic optical cavity for atom detection and manipulation,” *European Physical Journal D*, 53(1), 107-111 (2009).
- [13] Hibbs-Brenner, M.K. and Sullivan, C.T., “Low-loss AlGaAs optical rectangular waveguides at 830 nm”, *Applied Physics Letters*, 56(16) 1529-1531 (1990).